JOURNAL OF SOLID STATE CHEMISTRY 35, 334–340 (1980)

An Investigation of the Structure of 12HBaCoO$_{2.6}$ by Electron Microscopy and Powder Neutron Diffraction

A. J. JACOBSON

Exxon Research and Engineering Company, P. O. Box 45, Linden, New Jersey 07036

AND J. L. HUTCHISON

Department of Metallurgy, Parks Road, Oxford OX13QR, England

Received August 27, 1979; in revised form March 6, 1980

A combination of high-resolution electron microscopy and profile analysis of powder neutron data has been used to determine the structure of the perovskite-related phase 12HBaCoO$_{2.6}$. The structure is based on a 12-layer stacking sequence $(ccchhh)_2$ (space group $P6_3/mmc$). The oxygen vacancies were found to be nonrandom and are introduced by the replacement of some BaO_3 layers by BaO_2 layers of the type found in $Ba_3V_2O_8$.

Introduction

The anion-deficient perovskite-related phases ABO_{3-x} (A = Ca, Sr, Ba; B = Mn, Fe, Co, Ni) have structures based on close-packed AO_3 layers with B cations in octahedral interstices. Relationships between the ranges of nonstoichiometry of these phases and the stacking sequences adopted are complex. For example, in the system $Ba_{1-y}Sr_yMnO_{3-x}$ seven oxygen-deficient phases are found whose stability depends on the values of both x and y (*1*). Structural studies of 4H(Ba,Sr)MnO_{3-x} (*2*) and 6HBaFeO_{3-x} (*3*) by neutron diffraction have shown that the oxygen vacancy distribution in these compounds is related to a preference to adopt trigonal bipyramidal coordination for Mn^{3+} and tetrahedral coordination for Fe^{3+}. The site preference of the reduced cation in part determines the stacking sequence. Here we report an extension of this work to the system $BaCoO_{3-x}$. The reduced cation in this case, $Co^{3+}(d^6)$, has a strong site preference for octahedral coordination but the higher oxidation state $Co^{4+}(d^5)$ is found in both octahedral and tetrahedral sites. Phase relationships for $BaCoO_{3-x}$ have been investigated by several authors. Zanne *et al.* (*4*) prepared compounds at 905°C at different partial oxygen pressures and identified 2HBaCoO_{3-x} ($2.85 < 3 - x < 3.0$), 7H ($2.52 < 3 - x < 2.575$), 12H ($2.43 < 3 - x < 2.49$), 15H ($2.10 < 3 - x < 2.23$), an orthorhombic phase $BaCoO_{2.07}$ and $BaCoO_2$. All are perovskite related except $BaCoO_2$ and apart from the 2H phase have unknown structures. The starting material used was prepared at 1200°C but similar results were obtained with material prepared at 900°C except for 2H which showed a monoclinic supercell possibly as a consequence of long-range ordering. Negas and Roth (*5*)

0022-4596/80/150334-07$02.00/0

investigated $BaCoO_{3-x}$ in air as a function of temperature and observed only the 2H compound below 890°C. Between 890 and 925°C a slow transformation of 2H to 12H occurred and above 925°C an orthorhombic phase was formed with a powder pattern similar to that reported for $BaCoO_{2.07}$ (*4*). Negas and Roth also found a sharp discontinuity in the 2H lattice parameters at 740°C and some evidence for a superstructure between 740 and 890°C. Greaves (*6*) studied $BaCoO_{3-x}$ as a function of p_{O_2} and found evidence for the existence of several ordered intermediates with large orthorhombic supercells of 2H. His results confirm the existence of the 12H structure.

At this time, the detailed phase relationships with respect to oxygen nonstoichiometry, vacancy ordering, and structure are not fully understood. However, the existence of the 12H phase is well established and a detailed structural study of this compound should give some insight into the structural principles involved in the reduction of $BaCoO_3$. Single crystals of $12BaCoO_{3-x}$ have not been prepared, partly because of its narrow range of stability in air and also because the 2H to 12H transformation is slow. There are 42 possible hexagonal stacking sequences of 12 close-packed layers and consequently the determination of the structure from powder diffraction data would involve much computation.

We have recently shown (*7*, *8*) that high-resolution electron microscopy can be directly correlated with stacking sequences in perovskite-related compounds. This technique has been used to obtain a trial solution for further structural analysis of powder neutron diffraction data. A preliminary account of this work has been given (*9*).

Experimental

Sample Preparation

A stoichiometric mixture of $BaCO_3$ and Co_3O_4 (Johnson Matthey "Specpure" Chemicals) was hand mixed in an agate mortar and then fired in a platinum crucible at 905°C in air. A Philips X-ray diffractometer with monochromated Cu$K\alpha$ radiation was used to follow the progress of the reaction. After three initial firings and two intermediate regrinds, there was no unreacted $BaCO_3$ and the $BaCoO_{3-x}$ phase present was predominately 2H; the strongest lines of the 12H phase $(10\bar{1}7)$ and $(11\bar{2}0)$ could just be detected. The sample was then annealed for a total of 90 days to effect the slow 2H to 12H conversion. The sample was periodically quenched and the progress of the reaction monitored by X-ray diffraction. After 90 days a small amount of 2H remained but further annealing produced no further conversion, suggesting that some transformation back to 2H was occurring during the time taken to quench the large (25 g) sample necessary for the neutron diffraction experiment. The amount of 2H phase present was estimated from the neutron data (see below). The mean cobalt oxidation state was determined by adding the solid material to HCl containing an excess of KI and titrating the liberated I_2 with $Na_2S_2O_3$. The composition was found to be $BaCoO_{2.61(4)}$.

Electron Microscopy

Lattice images of thin crystals mounted on carbon-coated Cu grids were obtained with a Siemens Elmiskop 102 electron microscope. The accelerating voltage was 100 keV and images were obtained at magnifications of 500,000 × with a 40-μm objective aperture which included beams out to 0.3 Å^{-1}. The electron beam was along $(10\bar{1}0)$. The projections of several 12-layer sequences were compared with the lattice image shown in Fig. 1 and the best correlation was found to be with $(ccchhh)_2$ or in Zhadanov notation (*10*) $|1(4)1|1(4)1|$. An idealized projection of this sequence is shown inset in Fig. 1.

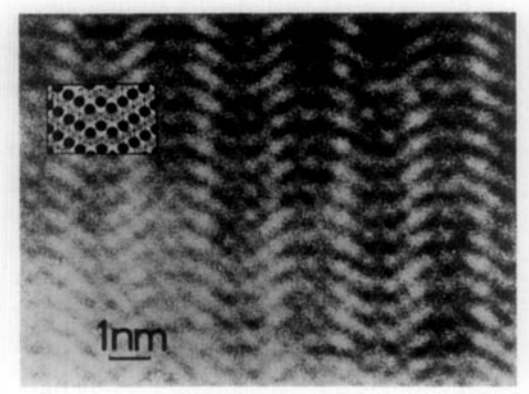

FIG. 1. Lattice image of $BaCoO_{2.61}$ with the electron beam alongc(10$\bar{1}$0).

Neutron Diffraction

Neutron diffraction data were collected at 4.2 K on a powder diffractometer at UKAEA Harwell with a wavelength of 1.5423 Å from the (511) planes of a Ge monochromator with a takeoff angle of 90°. The counter was stepped at 0.02° and accumulated counts printed at 0.1° intervals over the angular range $7° < 2\theta < 85°$. The sample was contained in a thin-walled 16-mm-diameter vanadium can in a vanadium-tailed cryostat.

The structure was refined by the profile analysis method (*11*) with starting positions corresponding to the sequence $(ccchhh)_2$ deduced from the lattice image. The space group is $P6_3/mmc$ and the scattering lengths used were $b_{Ba} = 0.52 \times 10^{-12}$ cm, $b_O = 0.58 \times 10^{-12}$ cm (*12*), and $b_{Co} = 0.252 \times 10^{-12}$ cm (*13*). Background contributions were estimated and an overall isotropic temperature factor was assumed. The distribution of oxygen vacancies was initially taken to be random.

Refinement of all parameters except the oxygen occupation numbers gave a high R value. When the oxygen occupation numbers were included the R value improved somewhat but was still unacceptably high (R profile, 32.8%; R expected, 10.4%) and the O atom occupancy in the central cubic layer O(1) refined to zero. Further refinement of all occupancies with a fixed scale factor revealed a major discrepancy for only O(1) and not Ba(1) in the same layer. It seemed likely that the stacking sequence was correct in that the oxygen vacancy distribution was nonrandom. The O(1) atoms initially in 6*g* positions were consequently started in 4*f*. The change in O(1) from 6*g* to 4*f* positions gives Co(1) tetrahedral rather than octahedral coordination. The refinement with this adjustment in the starting positions led to a profile R factor of 20.3% and plausible values for all the oxygen occupation numbers. A number of small discrepancies, however, still remained in the difference of the observed and calculated profiles. The origin of most of these was clearly the presence of the small amount of 2H known to be present from the X-ray diffraction data. The amount of 2H was estimated to be 7% from a calculation of the profile and the observed intensities of the 2H (20$\bar{2}$1), (10$\bar{1}$2), and (22$\bar{4}$0) reflections. The parameters for the 2H structure used for the calculated profile were taken from Ref. (*14*). Three small regions in the profile corresponding to the strongest 2H reflections were excluded in subsequent refinements.

The small discrepancies in the intensities on three low-angle reflections were considered to be most likely magnetic in origin. With this assumption various models for a magnetic structure were investigated with spin directions parallel and perpendicular to the c axis and different combinations of ferromagnetic and antiferromagnetic coupling between layers. Since no reflections were observed which could not be indexed on the chemical cell, the magnetic unit cell was assumed identical. The limited number of observations of magnetic reflections and their low intensities made a precise determination of the magnetic structure impossible. It was found, however, that the inten-

sities of the $(10\bar{1}3)$ and $(10\bar{1}5)$ reflections could only be reproduced with a model involving ferromagnetic coupling of the Co (1) sites. All models with ferromagnetic coupling of these cobalt atoms gave a value for gS close to 3.2 and small values for moments on the other cobalt sites, typical $gS = 1$. Models with the Co(1) atoms coupled antiferromagnetically gave substantially higher profile R factors and clear discrepancies in the difference profile. The final refinement of the data with the best model for the magnetic structure is shown in Fig. 2. In this refinement the spin direction was along the c axis and the R factors were R (profile) = 15.9%, R (expected) = 10.4%, R (nuclear intensities) = 6.8%, and R (magnetic intensities) = 18.2%. The high R factor for the magnetic intensities is indicative of the uncertainty in the magnetic structure. It is important to note that the atom positions are not significantly influenced by this uncertainty since the magnetic peaks fall off rapidly in intensity with increasing $\sin\theta/\lambda$ and are weak even at low angle. Atom positions and oxygen occupation numbers, for example, agree within one standard deviation for models with the spin direction parallel and perpendicular to the c axis. Atom positions and occupation numbers are given in Table I; the final parameter shifts were less than 0.3σ. The refined lattice parameters were $a = 5.761$ (1) Å and $c = 28.545$ (6) Å. Interatomic distances and angles are given in Table II. Cobalt has a much smaller scattering length than either barium or oxygen and consequently the cobalt positions are the least well determined. This is reflected in greater errors in the Co–O and Co–Co distances.

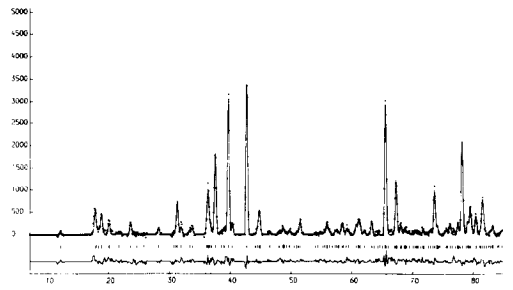

FIG. 2. Powder neutron diffraction profile for Ba $CoO_{2.61}$ at 4.2 K. Small circles are the experimental points, and the continuous line passes through the calculated points. The small vertical lines mark the positions of the Bragg reflections and the bottom trace is the difference profile.

TABLE I

ATOM POSITIONS AND OCCUPATION NUMBERS FOR $BaCoO_{2.6}$

Atom	Pos.	x	y	z	N
Ba(1)	$2a$	0	0	0	0.5
Ba(2)	$4f$	$\frac{2}{3}$	$\frac{1}{3}$	0.0950(5)	1.0
Ba(3)	$4f$	$\frac{1}{3}$	$\frac{2}{3}$	0.1758(4)	1.0
Ba(4)	$2d$	$\frac{2}{3}$	$\frac{1}{3}$	$\frac{1}{4}$	0.5
Co(1)	$4f$	$\frac{1}{3}$	$\frac{2}{3}$	0.0581(8)	1.0
Co(2)	$4e$	0	0	0.1226(11)	1.0
Co(3)	$4e$	0	0	0.2072(13)	1.0
O(1)	$4f$	$\frac{1}{3}$	$\frac{2}{3}$	−0.0042(5)	0.88(3)
O(2)	$12k$	0.1647(13)	0.3294(26)	0.0811(3)	2.81(6)
O(3)	$12k$	0.8572(9)	0.7144(18)	0.1663(4)	2.75(7)
O(4)	$6h$	0.1513(15)	0.3026(29)	$\frac{1}{4}$	1.53(4)

Note. a = 5.671(1), 28.545(6) Å.

TABLE II

BOND DISTANCES AND ANGLES IN $BaCoO_{2.6}$

Ba(1)–O(1)	3.276(4)	Co(1)–O(1)	1.778(15)
Ba(1)–O(2)	3.815(5)	Co(1)–O(2)	1.797(15)
Ba(2)–O(2)	2.864(5)	Co(2)–O(2)	1.978(17)
Ba(2)–O(3)	2.767(4)	Co(2)–O(3)	1.890(17)
Ba(3)–O(2)	3.176(6)	Co(3)–O(3)	1.828(21)
Ba(3)–O(3)	2.858(5)	Co(3)–O(4)	1.923(21)
Ba(3)–O(4)	2.766(7)	Co(3)–Co(2)	2.453(20)
Ba(4)–O(3)	3.034(3)	Co(3)–Co(3)	2.407(22)
Ba(4)–O(4)	2.839(6)	O(3) –O(3)	3.253(4)
O(1) –O(2)	2.952(7)	O(3) –O(3)	2.418(6)
O(2) –O(2)	2.770(8)	O(3) –O(4)	2.790(7)
O(2) –O(3)	2.866(6)	O(4) –O(4)	2.598(9)
O(2) –O(2)	2.901(8)	O(4) –O(4)	3.073(8)

O(1)–Co(1)–O(2)	111.3	O(3)–Co(3)–O(3)	82.8
O(2)–Co(1)–O(2)	107.6	O(3)–Co(3)–O(4)	96.1
O(2)–Co(2)–O(3)	95.6	O(4)–Co(3)–O(4)	85.0
O(3)–Co(2)–O(3)	79.6		

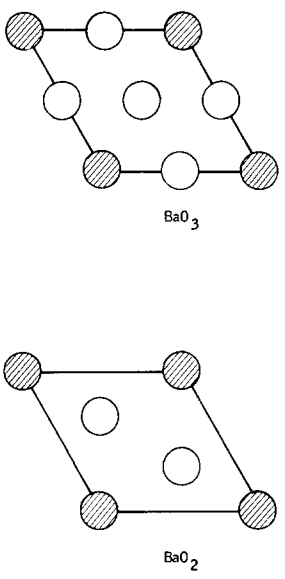

FIG. 3. Arrangement of bariums and oxygens in BaO_3 and BaO_2 layers.

Discussion

The structure of $12HBaCoO_{2.61}$ is based on the BaO_3 stacking sequence $(ccchhh)_2$ but one-sixth of the BaO_3 layers are replaced by BaO_2 layers (Fig. 3). As a consequence of this ordered arrangement of vacancies one-third of the cobalt atoms are tetrahedrally coordinated by oxygen. The CoO_4 tetrahedra are corner joined to strings of four face-shared octahedra containing the remaining cobalt ions (see Fig. 4). If it is assumed that the tetrahedral sites contain only cobalt(IV) and the octahedral sites only cobalt(III), then the ideal composition is $BaCoO_{2.67}$, in agreement with the composition determined by chemical analysis, $BaCoO_{2.61(4)}$, and by refinement of the oxygen, site occupancies, $BaCoO_{2.59(7)}$. However, the introduction of only two BaO_2 layers into the 12-layer structure provides too few oxygen vacancies and additional vacancies must be accommodated in BaO_3 layers. The required composition of the BaO_3 layers is $BaO_{2.8}$. Vacancy concentrations on this level can be tolerated in face-shared octahedra in the $BaCoO_{3-x}$ system as evidenced by the formation of $2HBaCoO_{3-x}$ with $2.85 < 3 - x < 3.0$ at 900°C (*4*).

Occupation of the tetrahedral sites by Co(IV) is supported by a comparison of the measured bond distances with those for other tetrahedral Co(IV) systems. The average tetrahedral Co–O distance in $12HBaCoO_{2.61}$ is 1.79 Å which may be compared with average values of 1.78 and 1.81 Å for Ba_2CoO_4 (*15, 17*) and Na_4CoO_4 (*16*), respectively. The average octahedral Co–O distance is 1.90 Å, although there are appreciable variations from octahedron to octahedron (1.83–1.98Å). Co(III)–O bond distances from ionic radii (*18*) are predicted to be 1.895 and 1.96 Å for low- and high-spin Co(III), d^6, respectively, in reasonable agreement. The Co–O distance found from the single-crystal

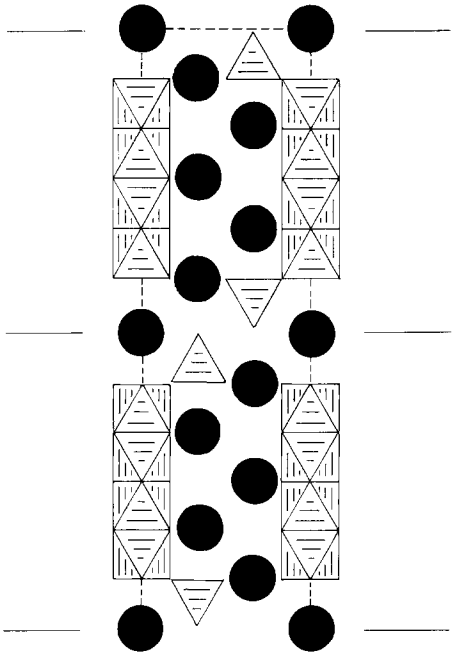

FIG. 4. Idealized $(11\bar{2}0)$ projection of the structure of $BaCoO_{2.61}$; Ba, ●; CoO_4 tetrahedra ▽; CoO_6 octahedra ▽

X-ray diffraction study of 2HBaCoO$_3$ (*14*) is somewhat shorter, 1.87 Å, but the exact composition of this crystal is not known.

The local cobalt environments are shown in Fig. 5. The Co(2)–O(2) distance is apparently lengthened to compensate for the short Co(1)–O(2) distance in the CoO_4 tetrahedron. The Co(2)–Co(3) distance is longer than the Co(3)–Co(3) distance, suggesting a relaxation of the terminal cobalts in the face-shared string to minimize Co–Co electrostatic repulsions across the shared octahedral face. Co–Co repulsions are further screened by the three face-shared oxygens which form short O–O distances. Short O–O distances are usually observed in ABO_{3-x} systems with hexagonal stacking, for example, 2.511 Å in 2HBaCoO$_3$ (*14*), 2.448 Å in 6HBaFeO$_{2.79}$ (*3*), and 2.507 Å in 8HBaMnO$_3$ (*19*).

The replacement of BaO_3 by BaO_2 layers leading to tetrahedral cation coordination is not unique to 12HBaCoO$_{2.61}$. Longo and Clavenna (*20*) have pointed out that mixed metal oxides $A_3B_2O_8$ with the palmierite structure can be similarly described. In these structures the *B* cation is always tetrahedrally coordinated and the structure is closely related to 9RBaRuO$_3$. One-third of the BaO_3 layers in $BaRuO_3$ become BaO_2 layers, and the BaO_2 layers convert the terminal octahedra of the string of three face-shared octahedra to tetrahedra containing the *B* cation; the central octahedral site is vacant. The palmierite and 12HBaCoO$_{2.6}$ structures both provide ways of accommodating cations with a strong site preference for tetrahedral coordination while largely maintaining the high lattice energy of a nearly close-packed AO_3 framework.

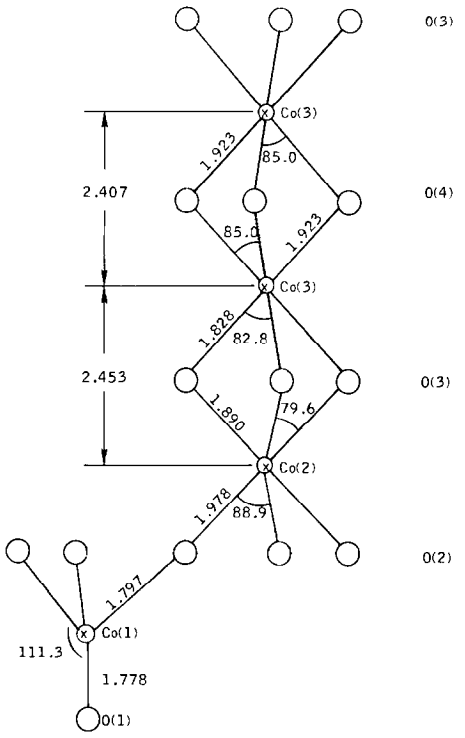

FIG. 5. Co environment in BaCoO$_{2.61}$.

Acknowledgments

We thank Professor J. S. Anderson for his interest in this work and the Science Research Council for financial support.

References

1. T. NEGAS, *J. Solid State Chem.* **6**, 136 (1973).
2. A. J. JACOBSON AND A. J. W. HORROX, *Acta Crystallogr. Sect. B* **32**, 1003 (1976).
3. A. J. JACOBSON, *Acta Crystallogr. Sect. B* **32**, 1087 (1976).
4. M. ZANNE, A. COURTOIS, AND C. GLEITZER, *Bull. Soc. Chim. Fr.* 4470 (1972).
5. T. NEGAS AND R. S. ROTH, NBS Special Publication 364, 1972.
6. J. R. GREAVES, "Thermodynamic Properties of Mixed Metal Oxides," D. Phil. thesis, Oxford University, England, 1969.
7. J. L. HUTCHISON AND A. J. JACOBSON, *Acta Crystallogr. Sect. B* **31**, 1442 (1975).
8. J. L. HUTCHISON AND A. J. JACOBSON, *J. Solid State Chem.* **20**, 417 (1977).
9. A. J. JACOBSON AND J. L. HUTCHISON, *J. Chem. Soc., Chem. Commun.* 116 (1976).
10. A. L. PATTERSON AND J. S. KASPER, *in*

"International Tables for X-ray Crystallography," Vol. II, p. 342, Kynoch Press, Birmingham, 1972.
11. H. M. RIETVELD, *Acta Crystallogr.* **22,** 151 (1967).
12. Neutron Diffraction Commission, *Acta Crystallogr. Sect. A* **28,** 357 (1972).
13. C. INFANTE, "Neutron Scattering Studies of Transition Metal Oxides," D. Phil. thesis, Oxford University, England, 1976.
14. H. TAGUCHI, Y. TAKEDA, F. KANAMARU, M. SHIMADA, AND M. KOIZUMI, *Acta Crystallogr. Sect B* **33,** 1299 (1977).
15. H. MATTAUSCH AND H. MULLER-BUSCHBAUM, *Z. Anorg. Allg. Chem.* **386,** 1 (1971).
16. M. JANSEN, *Z. Anorg. Allg. Chem.* **417,** 35 (1975).
17. G. A. CANDELA, A. H. KAHN, AND T. NEGAS, *J. Solid State Chem.* **7,** 360 (1973).
18. R. D. SHANNON, *Acta Crystallogr. Sect. A* **32,** 751 (1976).
19. A. D. POTOFF, B. L. CHAMBERLAND, AND L. KATZ, *J. Solid State Chem.* **8,** 234 (1973).
20. J. M. LONGO AND L. R. CLAVENNA, *Ann. N.Y. Acad. Sci.* **272,** 45 (1976).